The High Cycle Fatigue, Deformation and Fracture ofCompacted Graphite Iron:Influence of Temperature

C.L. Zou, J.C. Pang, M.X. Zhang, Y. Qiu, S.X. Li, L.J. Chen, J.P. Li, Z. Yang, Z.F. Zhang

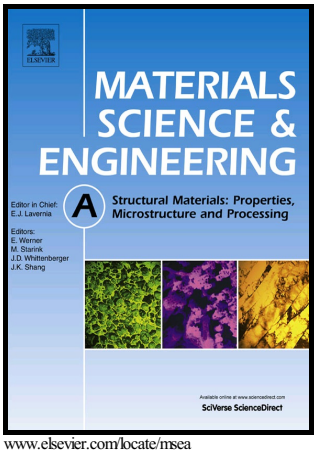

www.elsevier.com/locate/msea

PII: S0921-5093(18)30026-1
DOI: https://doi.org/10.1016/j.msea.2018.01.025
Reference: MSA35979

To appear in: *Materials Science & Engineering A*

Received date: 29 August 2017
Revised date: 25 December 2017
Accepted date: 5 January 2018

Cite this article as: C.L. Zou, J.C. Pang, M.X. Zhang, Y. Qiu, S.X. Li, L.J. Chen, J.P. Li, Z. Yang and Z.F. Zhang, The High Cycle Fatigue, Deformation and Fracture ofCompacted Graphite Iron:Influence of Temperature, *Materials Science & Engineering A,* https://doi.org/10.1016/j.msea.2018.01.025

The High Cycle Fatigue, Deformation and Fracture ofCompacted Graphite Iron:Influence of Temperature

C. L. Zou[a, b], J. C. Pang[b, *], M. X. Zhang[b] , Y. Qiu[b], S. X. Li[b], L. J. Chen[a], J. P. Li[c], Z. Yang[c], Z. F. Zhang[b,*]

[a] School of Materials Science and Engineering, Shenyang University of Technology，111 Shenliao Road, 110870, Shenyang, PR China

[b]Shenyang National Laboratory for Materials Science, Institute of Metal Research, Chinese Academy of Sciences, 72 Wenhua Road, Shenyang 110016, PR China

[c]School of Materials and Chemical Engineering, Xi'an Technological University, 2 Xuefuzhong Road, 710021, Xi'an, PR China

Abstract:

The microstructure, tensile strength, high-cycle fatiguepropertyand corresponding damage mechanisms of compacted graphite iron at room temperature (25 ^{o}C), 400^{o}C and 500^{o}C, were investigated. It is found that the fatigue strength increases at first and then decreases with the increase of the testingtemperature.At 25^{o}C,the fatigue crackmainlyinitiatesfrom graphite debonding and propagates along the graphiteclusters.At 400 ^{o}C,the fatigue crack initiationis influenced by oxidation; the fatigue strengthmay be improved by dynamic strain aging.At 500^{o}C, theoxidation becomes more serious andthe oxide layer accelerates the crack to propagate along the matrix. At the same time, the phenomenon of grain boundarysoftening, one of the reasons resulting in the reduction of fatigue strength,is found.Then, the model ofdamage mechanismwas proposedaccording to the propagation behavior of fatigue crack at high temperatures, and the quantitative relationship betweenthefatigue strength and the ratio of the interphase corrosion depth to the critical crack lengthwas established.This investigationmay enrich the fundamental understandingon the damage mechanism of compacted graphite iron.

Key words: Compacted graphite iron;Testing temperature; High-cycle fatigue property; Oxidation effect;Dynamic strain ageing.

*Corresponding authors. E-mail address:jcpang@imr.ac.cn (J. C. Pang); zhfzhang@imr.ac.cn (Z. F. Zhang).

1. Introduction

Compacted graphite iron as an important engineering material, has excellent castability, wear resistance,moderate thermal conductivity andmechanical properties between nodular cast iron and gray cast iron[1, 2]. Owing to the excellent coupling properties of mechanical and physical ones, the compacted graphite iron is extensively used in cylinder head of diesel engine with high power. However, in recent years, the engine working temperature usually increases in order to improve the combustion efficiency and generate a reduction of pollution[3],which put higher demand on material performances.In particular, the high-cycle fatigueproperty is akey forcompacted graphite iron, because the operation of the diesel engine will cause a high frequency impact of high pressure gas anda high speed periodic variation in the internal stress field, and then result in component fatigue failure.As is well known thatinhigh-cycle fatigue the local plastic deformation will appear, it is difficult to effectively prevent the fatigue failure. In addition, the effect of temperature on the fatigue property of compacted graphite iron is crucial, and finite element analysis indicated that the distribution of temperatures on the flame deck surface of the cylinder head is from 37^{o}C to 497^{o}C[4]. The mechanicaland oxidation resistancepropertiescould become sensitive at a high temperature[5],which results in the completely different failure mechanism from the room temperature. Therefore, it is necessary to investigate the fatigue damage mechanism of compacted graphite ironathightemperature.

In the last few years,themechanical property of compacted graphite ironhas drawn many public attentions.The tensile properties and damaging mechanisms of compacted graphite irons at different temperatures have been compared in the previous studies[6-9]. Itisshown that the tensile strength decreasesslightly at firstwith the increase of testing temperature, and then dramatically.This is mainly influencedby dislocation strengthening and grain boundary softening.In these studies the effects of oxidation were not taken into account because the tensile test takes short time.However, the trend of the fatigue property with temperatureis quite differentfrom

tensile property due to the long-term loading.A large number of studies[10, 11]indicate that:thefatigue strength of compacted graphite ironincreasesfirstly and thendecreasesas the temperature increases from 200^{o}Cto 400^{o}C;when the temperature rises further, itdecreases rapidly. The occurrence of peak fatigue strengthis probably due to the immobilizationof mobile dislocations caused by carbon atoms[12].However, the decreasing reason of fatigue strength has no reasonable explanation so far. In addition, the oxidation appears inevitably in the practical application of compacted graphite iron.According to the references[13-16], the oxidation of the sample surface and the crack tipwasextensively observedduring thermo-mechanical fatigue.The oxide layer induces the crack propagation in the matrix, accelerates the crack growth, and finally leads to the failure.However,oxidation or dynamic strain aging can more effectively affect the damagemechanisms of the crack tip at high temperatures.Therefore, more systematic and deeper investigationsshould be carried out for a reasonable explanation.

In the presentstudy, the evolution tendencies of thehigh-cycle fatigueproperties of compacted graphite ironat the temperatures including 25^{o}C, 400^{o}C and 500^{o}Cwereinvestigated, and then the corresponding failure modeand damage mechanismwerediscussed.

2. Experimental materials and procedures

Theinvestigated materialwasCast RuT400 (Chinese designation of compacted graphite iron) witha cuboidalshape. The composition of compacted graphite iron is shown in Table 1.The tensile and fatigue specimenswere cut into the same shape and size as shown in figure1.The specimens were polished with #800, #1200 and #2000 emery papers in sequential order along the longitudinal direction.Tensile tests were conductedat strain rate of 5×10^{-4}s byahydraulic servo testing machine Instron 8862.The stress controlledaxialpull-push fatigue tests with stress ratio of R=-1 were performed on the RumulTestronic 100 kNelectromagnetic resonant testing machine.A sinusoidal waveform in the frequency of about 80-110Hz was used.The fatigue strength (σ_{-1}) ofthe specimens defined as the stress amplitude at which can endure the

10^7cycles,was determined by staircase method.Before the tensile and fatigue testsat high temperatures, the samples were incubated for half an hour to ensure uniform heating.

The metallographic specimensof compacted graphite ironwere observed withOLYMPUS 4000laser scanning confocal microscope (LSCM).Before observation, the specimens were etched with nital (4% HNO_3 in ethanol solution) for 20s. Area percentage of graphite, vermicularity, mean aspect ratio and average count of graphite particles in per square millimeter were measured with image pro plus (IPP). The specimen surface appearances and the fatigue fractographies were examined by JSM 6510 scanning electron microscopy (SEM) equipped with energy dispersive spectrometer (EDS).

Table 1

The chemical composition of compacted graphite iron (wt%).

C	Si	Mn	P	S	Cu	Sn	Fe
3.51~3.56	1.49	0.13	0.03	0.015	0.5	0.031	Balance

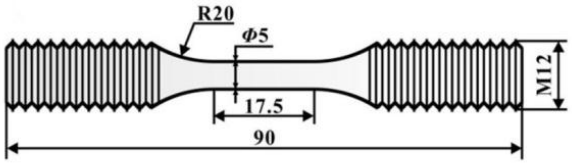

Figure1.The shape and dimension of tensile and fatigue specimens.

3. Experimental results

3.1 Microstructure

The optical microstructure is shown in figure2,it can be seen that the compacted graphite ironmainly consists of vermicular graphite, ferrite and pearlite.The area fraction of graphite is 8.01%, in the form ofvermicular and circular shapes. The vermicularity is about87.4% and the other part is spherical graphite. The spherical graphite generally distributes in pearlite zone and is surrounded by a thin ferrite, as shown in figure2awith the black arrow. The milky zone is equiaxed ferriteaccounting for 36.11% of the matrix area fraction which is usually divided into many clusters in the matrixas marked bygreen dotted lines in which many vermiculargraphites exist,

hereafter named as graphite cluster.Figure2b is high-magnification observations of the square area of figure2a, and the averagegrain size of the ferrite obtained by interception method, is about 12.6μm.The pearlite becomes gray-brown after corrosiondue to the poor corrosion resistance and the area fraction is55.85%.

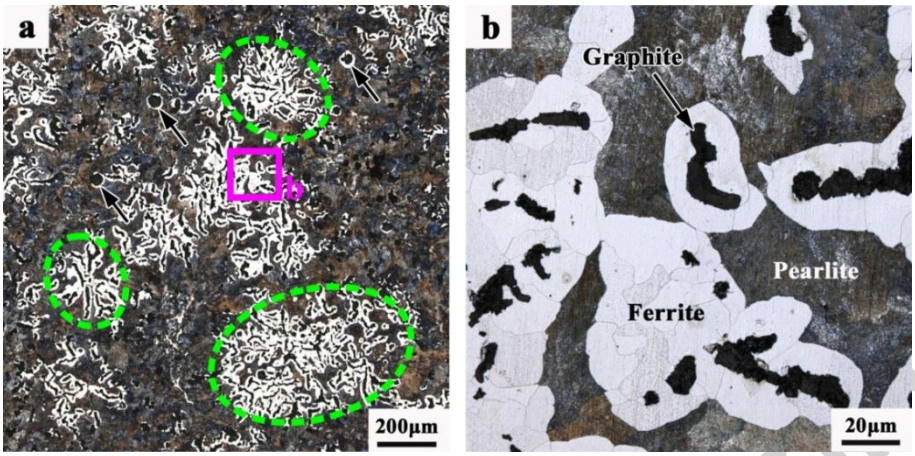

Figure2.(a)The microstructures of compacted graphite ironexamined with LSCM; (b) enlargement of the pink square areamarked in (a).

3.2 Tensile property

The tensile engineering stress-strain curves, strength andelongations to fracture ofcompacted graphite iron at 25^{o}C, 400^{o}C and 500^{o}C are shown in figure3. It can be seen that there is no obvious yield point in the tensile stress-strain curves at all temperaturesinvestigated,which is similar to the previous results[17]. The tensile strength decreases with the increase of temperature, which is 431MPa, 396MPa and 323MPa respectively (the black lineinfigure3b).In addition, with the increase of temperature, the elongation to fracture decreases slightly at first and then increases significantly (the blue lineinfigure3b). Theseare similar to the tendencyof other studies[18, 19]. Meanwhile,the serrated flowis observed at the yield stage ofstress-strain curvesat 400^{o}C and 500^{o}C, while does notoccur at 25^{o}C, due tothedynamic strain aging effectaccording to the studies[20, 21].The corresponding mechanism is usually interpreted as follows:the carbon atoms couldlock mobile edge dislocations,thereby the resistanceto further dislocationmovement increasesat aproper temperature range(about 200 ~400^{o}Cforiron-carbon alloy).

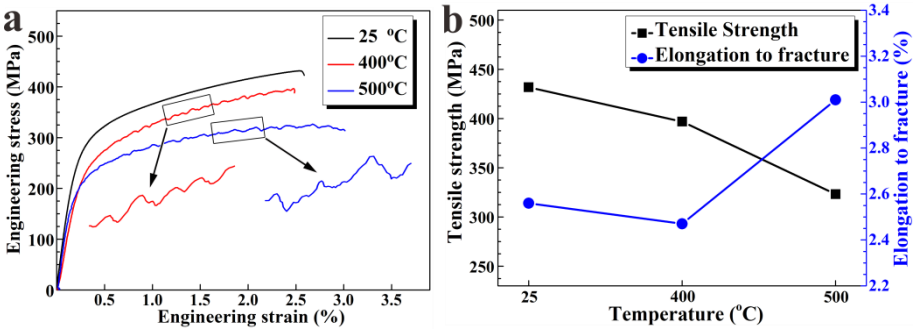

Figure3.Tensile properties of compacted graphite iron at different temperatures:(a)engineering stress-strain curves; (b) tensile strength and elongation to fracture.

3.3Fatigue property

Figure4shows the relationships between stress amplitude (σ_a) and the number of cycles to failure (S-N curves)at 25°C, 400°C and 500°Cand the fatigue strengthsare150MPa, 159MPa and 142 MPa,correspondingly.Obviously,the fatigue strength increases firstly and then decreases with the increase of temperatureas shown in figure 5a.

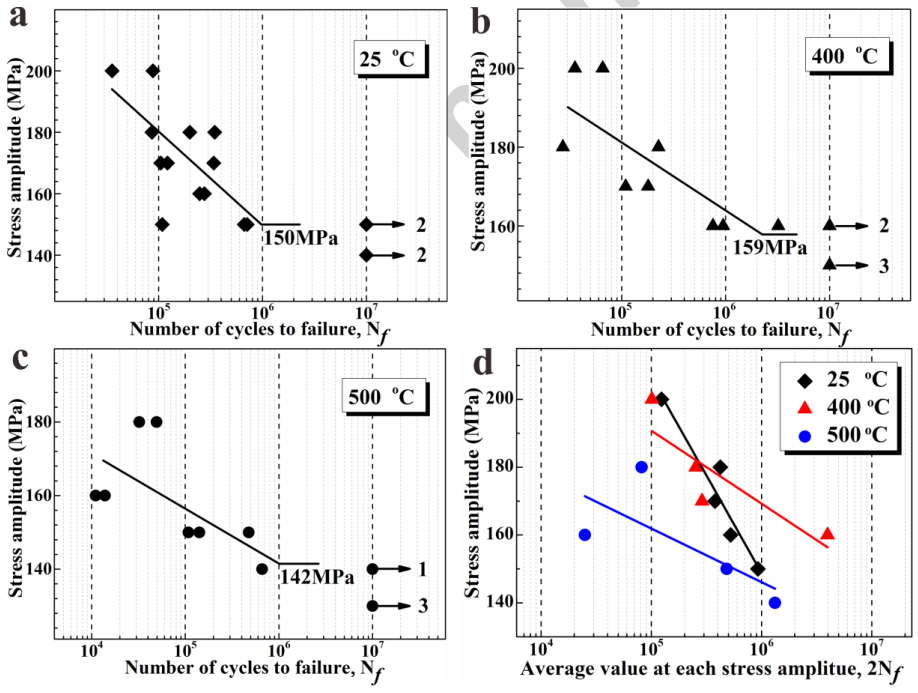

Figure4.Fatigue properties of compacted graphite iron at different temperatures:(a), (b) and (c)S-N curves;(d)stress amplitude - average value of$2N_f$ at each stress amplitude.

The Basquin equationis used to fitS-Ncurvesin the stress-controlled fatigue tests[22, 23], and shown as follows:

$$\log\sigma_a=\log\sigma_f'+b\log(2N_f) \quad (1)$$

where σ_f' is the fatigue strength coefficient,b is the fatigue strength exponent[10], and N_f is number of cycles to failure. It should be emphasized that the coefficient is closely related to the fatigue strength of smooth specimenand the exponent mainly reflects the cumulative fatigue damage rate of the material[24, 25].The stress amplitude vs. the average valueof $2N_f$ ateach stress amplitude under three temperaturesare shown in figure4d.The S-N curves at the three temperatures approximately exhibit a linear relationship in the logarithmic coordinate, and the fitting formulaat25^{o}C, 400^{o}C and 500^{o}Ccan be expressed as follows, respectively:

$$\log\sigma_a=2.67-0.08\log(2N_f)(2)$$

$$\log\sigma_a=2.46-0.04\log(2N_f)(3)$$

$$\log\sigma_a=2.34-0.03\log(2N_f)(4)$$

The fatigue strength coefficientsof compacted graphite iron specimensat 25^{o}C, 400^{o}C and 500^{o}Care 465, 287and 220MPa,respectively, as shown in figure5b (see blue data).This variation tendencycould be similar to the tensile strength (fatigue 3b). However,the valuesareobviously lower, especially at 400^{o}C and 500^{o}C.The fatigue strength exponentsincrease with increasing temperature (figures5bblack data),andare equal to -0.08, -0.04, and -0.03asobtained from equation(2)-(4).Normally, the value of b represents the damage rate of high-cycle fatigue[26, 27].Therefore,high-cycle fatigue damage rate of compacted graphite ironincreases with increasing temperature.

On the other hand, the fatigue strength exponentb is influenced by the change of fatigue crack initiation sites and the microstructures[9].These factors are usually much sensitive to the varietiesof stress amplitude.As a result, the fatigue lives show a large scatterwith the reduction of stress amplitudesin the S-N curves (see figures4a to4c).Based on the results above, itmaycome to the conclusionthat the temperature can obviously affect the fatigue strength of the compacted graphite iron.Therefore, it is necessary to further reveal the fatigue damage mechanisms at different temperatures.

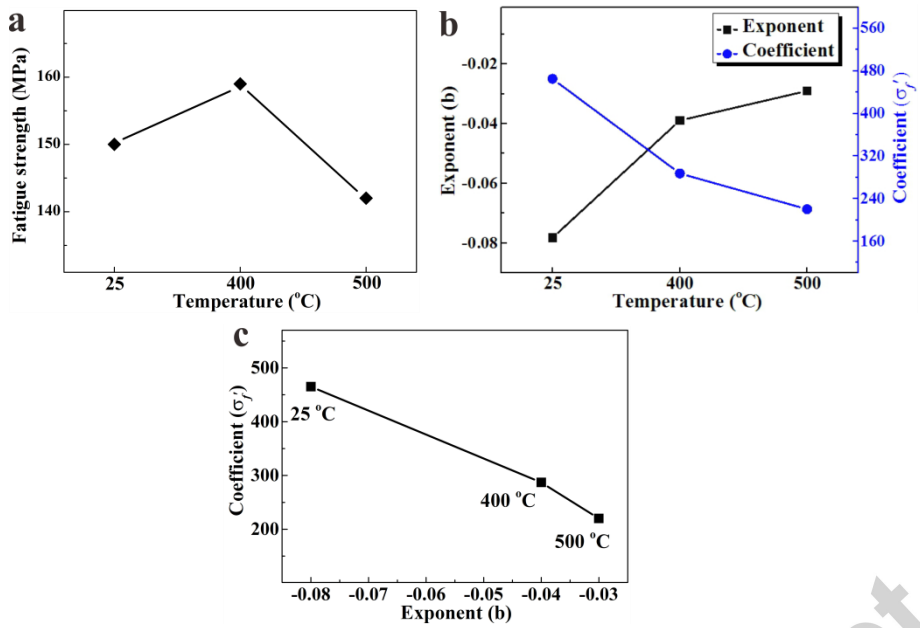

Figure5.The changes of fatigue strength(a),the fitting values of the parameters inBasquin equationat different temperatures (b) and the relationship of exponent and coefficient(c).

3.4 Fatigue fracture morphology

The SEM micrographs of the fracture surfaces at 25°C, 400°C and500°Cwereshown in figure6. Figures6(a), (c) and (e)showthemorphologies near the crack initiation sites. At 25°C,the crack initiation appears at the sample surface, and thecrack is induced by the vermicular graphite debonding in the cluster (figure6a).At 400°C,the crack initiation still appears at the sample surface;however,crack initiation site is at pearliteinstead ofvermicular graphite(figure6c).At 500°C, more obvious oxidation appears, and in the brittle oxide layerthe secondary cracks form under the cyclic stress (figure6e). These cracks may reduce the high-cycle fatigue life.Figures6(b), (d) and (f)show the slow crack propagation zonemorphologies. There aresome typical cleavage fracture patterns at 25°C and 400°C,indicating that the specimenundergoesbrittle fracture.However, someprecipitations of the carbide appear obviouslynear the crackswith cleavage fracture at 400°C(figure6d).Thesecarbides give rise to the pile up of dislocations and thus prevent the fatigue crack from propagation.At 500°C, there is no obvious cleavage pattern at the fracture surface, but a large number of intergranularcracks

exist. This may be due to the grain boundarysoftening at high temperature orthe preferential segregation of impurity elements at the grain boundaries[28].

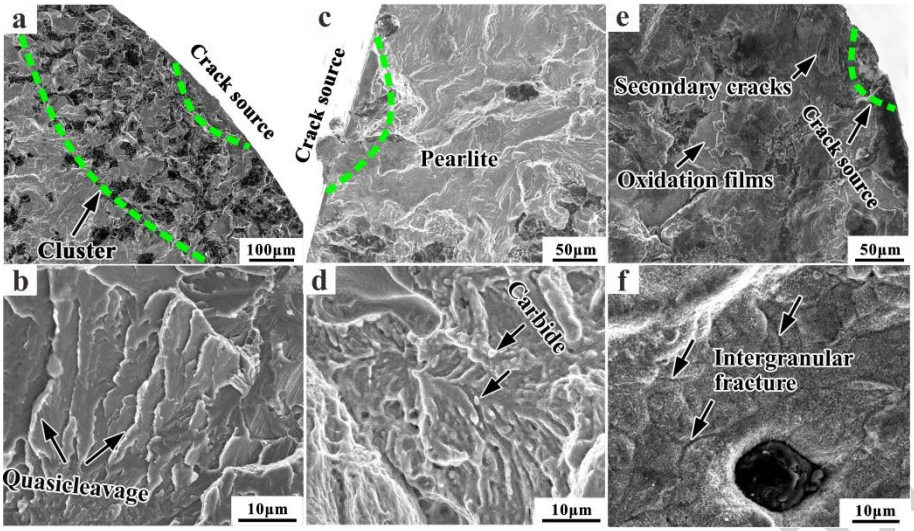

Figure 6.Fracture surface morphologies in crack initiation and slow propagation zones of the compacted graphite ironat different temperatures:(a) and (b) 25^{o}C, σ_a=160MPa, N_f =248258 cycles; (c) and (d) 400^{o}C, σ_a=160MPa, N_f=947720 cycles; (e) and (f)500^{o}C, σ_a=150MPa, N_f=108046 cycles.

3.5Crack growthand fractureprofiles

Figure 7 showsthe profiles of fatigue fracture at different temperatures. At 25^{o}C, it can be clearly seen that the fatigue crackinitiatesinferrite and propagates mainly along the graphitecluster. However, at 400^{o}C and 500^{o}C, the fatigue crack initiates in the pearlite and only propagates along a small number of graphite clusters. Obviously, the testing temperature may affect the crack initiation site of compacted graphite iron during high-cycle fatigue, which is consistent with the change of fatigue strength exponent.

The crack growth pathsat different temperaturesareshown in figure 8.It is noticed that manydiscontinuous and smaller crackscan be observed at room temperature,as shown infigures 8aandb,where the cracks initiate from graphiteand then propagate in the ferrite matrix around the graphite.The graphite is considered as a defectfor the crack initiation in the compacted graphite iron. While the micro-cracks are often prone to initiate at the tip of the graphite,which makes the main crack form and propagate along the graphitecluster.

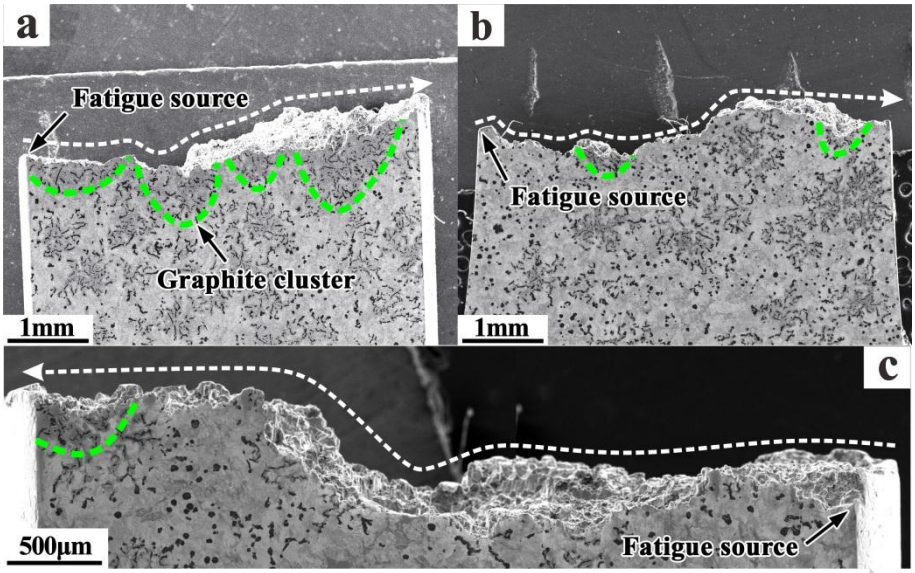

Figure 7.Profiles of fatigue fractureof compacted graphite iron at different temperatures: (a) 25^{o}C, σ_a =170MPa, N_f=104766 cycles; (b)400^{o}C, σ_a =200MPa, N_f=35522 cycles; (c)500^{o}C, σ_a =180MPa, N_f=49394 cycles.

The microstructuresaround the cracksat 400^{o}C and 500^{o}C are shown in figures 8c and drespectively.There is an obvious crack sourceinthe pearliteat the sample edge, whichimplies thatcrack iseasier tonucleate in the pearlite than in the graphite tip at high temperatures.Meanwhile,significantoxidationin the crack surfaceoccursat high temperature.At 400^{o}C, the oxide layer does not completely fillin the crack,and theresidual crevice causes the oxide layer to peel offthe surface of the crack.However, the oxide layer is full of the crackat 500^{o}C.It implies that the degree of oxidation is more serious than that at 400^{o}C.In addition,at 400^{o}C,the cracks can pass through thegraphite by two ways, one is thegraphiteinterior, and the other is phase boundary between graphite and ferrite.However,at 500^{o}C, the cracks onlypassthrough the phase boundary,which may be one of the reasons for the reduction in fatigue strength.

The partialenlargement of the micro-crack extension is showninfigure 9.It is apparent that the oxide layer uniformly covers on the surface of the sample at 400^{o}C, and the thickness is about 1.5μm, as shown infigure 9a. However,the oxide layer in the crack source is not continuous (see the arrows in figure 9a), which indicates that the oxide layer forms after the fatigue crack propagation.The initial crackpropagation direction is not perpendicular to the stress direction, but along the direction of the

pearlite lamellae.While during the subsequent propagation,the weak crack propagating along the pearlite lamellae reappears.Obviously, the pearlite lamellae play a certain role in the crackpropagation.

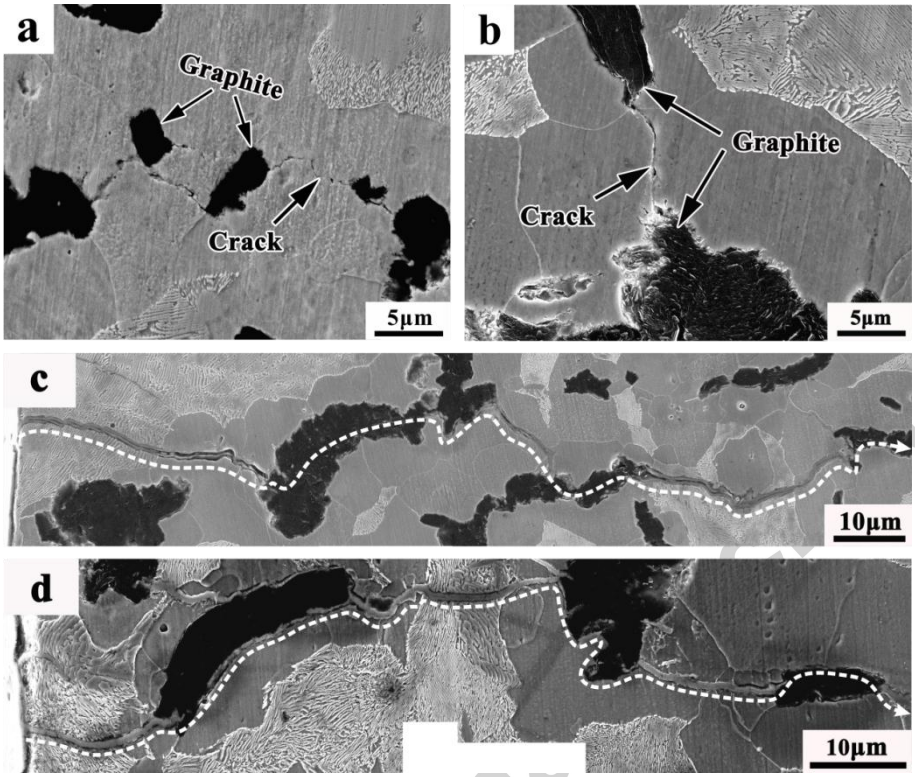

Figure 8.SEM micrographsalong main crack propagation path at different temperatures: (a) 25^{o}C, σ_a=160MPa, N_f=276287 cycles and (b) 25^{o}C, σ_a=200MPa, N_f=88202; (c) 400^{o}C, σ_a=170MPa, N_f=109053 cycles; (d) 500^{o}C, σ_a=180MPa, N_f=49394cycles.

At 500^{o}C,the thickness of the oxide layer on the sample surface is not uniform, and the thickest part is about 3μm, which is twice of that at 400^{o}C.The peeling of the oxide layerisa reason of uneven thickness.In addition, the oxide layer in the crack source is continuous, as shown in figure 9c. The crack mainly initiates from the oxide layerand thenpropagatesgradually toward the core.Therefore, it can be summarized that, at first, in the surface of the sample an oxide layerforms, then some cracks nucleate along the brittle oxide layerunder the cyclic stress, and gradually propagate into the matrix.Sometimes, the crackdeflectsalong the direction of the pearlitefor a short distance and then propagates mainly along the directionperpendicular to the stress.

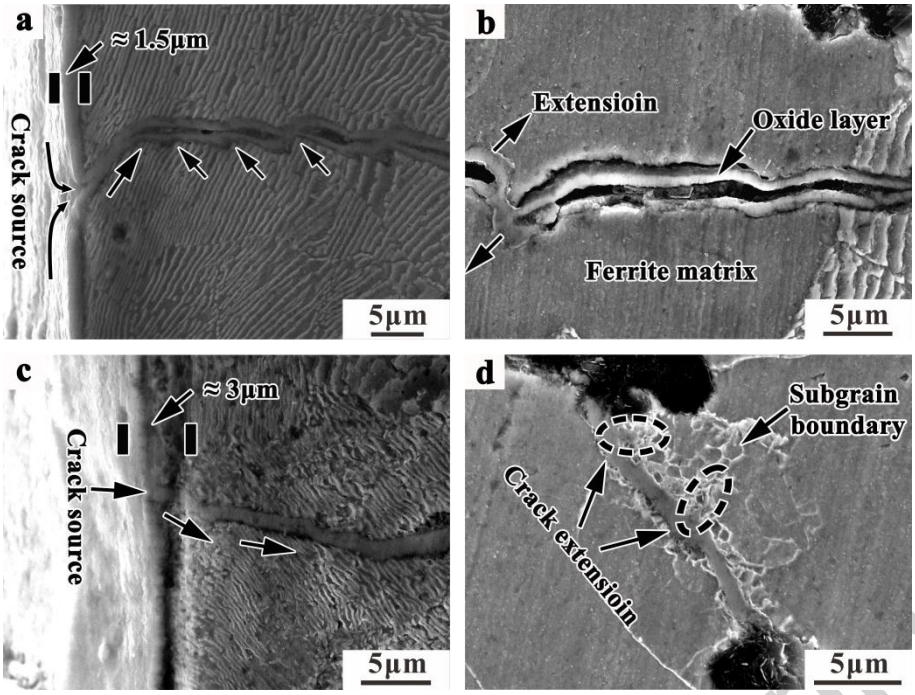

Figure 9.The microscopic morphologies of crack initiation and propagation at high temperatures: (a)and (b) 400°C, σ_a =170MPa, N_f=109053 cycles;(c) and (d) 500°C,σ_a =180MPa, N_f=49394 cycles.

Themorphologies of crackspropagation in ferrite at high temperaturesare shown infigures 9b and d. It can be seen that there isanapparentdebondingbetweenthe oxide scaleand the ferrite at 400°C, whichindicates thattheadhesion between the oxide layer and the ferrite of the compacted graphite iron is small.The ferrite does not continue to oxidize after debondingexcept for the part at the cornerwhere no debonding occurs (figure9b).Obviously,the gap between the oxide layer and the matrixcan effectively prevent the oxidationfrom extending.On the other hand, it is difficultto generatea crack inthe matrixeven if there isa micro-crack in the oxide layerifthe oxide layer has no direct contact with thematrix.

The crack in the ferrite at 500°C is shown infigure9d.It can be seen that there is no obvious debonding, because the crack is full of oxide layer resulting in insufficient space.The oxide layer is tightly attached to the matrixcausing cracks to propagate easily from the layer to thematrix,which is the prime formation reason for thesecondary cracks (black dashed circle in figure 9d)around the main crack.At the same time,it is commonly found a lot of subgrainscoarseningaround the main and

secondary cracks;whereas,thisphenomenoncan not be observed at 400°C.

4. Discussion

4.1 Fatigue damage mechanism

The aboveresultsdemonstrate thatthere are differentmodesforcrack propagationat25°C, 400°C and 500°C,as shown in figures 10-12,correspondingly.In the following, the fatigue damage mechanismswill be discussed in detail.

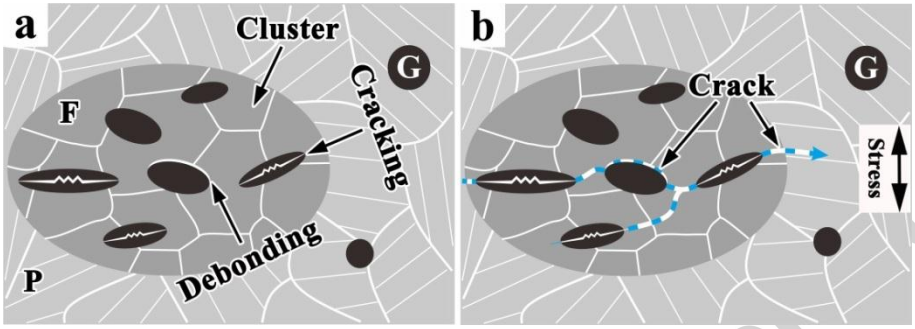

Figure 10.Schematic of crack formation and propagation at 25°C: (a) graphite debonding and cracking; (b) main crack forming.

At 25°C,the graphite withlow strength and poor ductilityiscurrentlyconsideredas the foremostdefect in compacted graphite iron[29].In this sense,whether the graphite debonding or crackingwill be affected bythe level of stress amplitude.On the other hand, the cracks may format theinterface because of poor bonding between graphite and matrix, as shown in figure 10a.Then, a plastic zone will form due to the stress concentration at the graphite tip and eventually develop into micro-cracks in the ferrite region.Then, they areconnected with each other to form the main crackin adjacentgraphite of the cluster, as shown in figure10b (the dotted line).

At 400°C, the oxidationinvadesthe matrixthroughpearlite lamellaein the form ofinterphasecorrosion between cementite and ferrite, as shown in figure 11a. According to the previous studies[30, 31], the corrosion rate of pearlite is much higher than ferrite due tointerphase corrosionin cast iron. This is the main reason for the crackinitiationin the pearlite at 400°C and 500°C.Due to the cyclic stress, the crack propagates along the pearlite lamellaeand turnstoperpendicular to the stress.At the same time, the surface of the sample comes into beingan oxide layer at high temperature. The oxide layerspreads along the edge of the crack to the matrix,as

shown infigures 11b and c.Noteworthily, the crack will becramped by thenext pearlite lamellae possibly by the ferrite plate and stoppropagatinguntil the oxide layer spreads along the crack edge to the tip, and the high stress and oxidation at the crack tip promote the crack extending to the ferrite plate (figure 11c)and then the interphase corrosion and cracking will happenagain, as shown in figure 11d. This is the reason for the appearance of "serrations"in figure9aas marked by smaller arrows.When the crack approaches to graphite, there are usuallytwo kinds of propagation paths, one is across the graphite, and the other is along the phase boundary between graphite and ferrite, as shown in figure 11d.

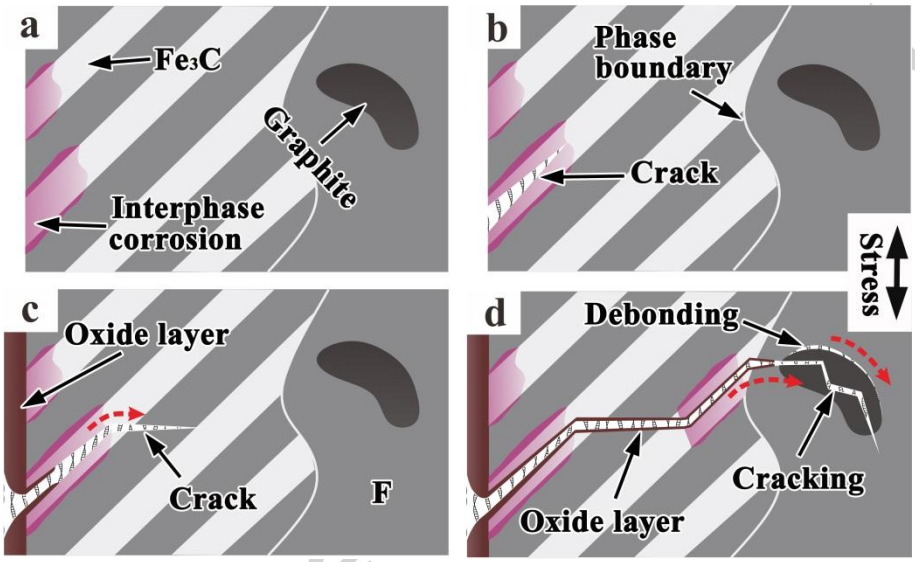

Figure 11.The illustration of crack formation and propagation at 400^{o}C: (a)interphase corrosion forming in pearlite lamellae; (b) crack forming in interphase corrosion region; (c) oxide layer forming onsample and crack surfaces;(d) the crack propagatingin the graphite.

At 400°C,the crackterminates in the pearlite regiongiving anindicationofblockingeffect of the pearlite lamellae on the crack,as shown in figure12a.The crack still has a tendency to propagate slightlyalongthe lamellae in thepearlite, as showninthe small black arrowsin figure12a.At the same time, a lot of carbides separate out in thepearlite lamellar.

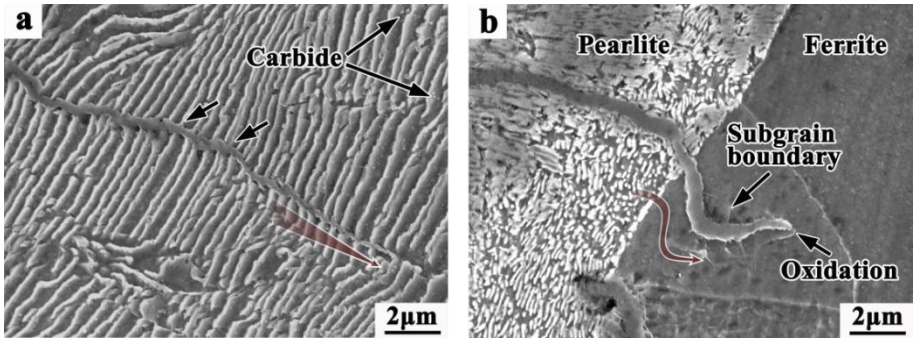

Figure12.The microstructuresaround crack tip: (a) 400^{o}C;(b) 500^{o}C.

Fromfigure 9c,it can be found that: at500^{o}C, the fatigue crack initiatesfrom pearlite, and it is undeniable that the interphase corrosionplays a certain rolein crack initiation.Furthermore,the oxidation degree is much serious thanthatat 400^{o}C, which must result in the formation of the oxide layer on thesample surfacefaster.In this case,thesurface oxide layeris too brittletoendure a largestrainleading to local cracking at first, as shown in figure9c and figure13b.Then,the oxygen atoms invade the matrix along the crack and a new oxide layer formsrapidlyat thefresh metalofthe crack tip.When the newoxide layercracks, a cycle of oxidation induced crack propagationwill end and the crack develops.As the crack propagates intothe matrix in the stress-controlled fatigue, thestressat the crack tipincreasesand then causes the oxidelayerto break.Therefore, the secondary cracksnucleate, propagate to thematrix, and then thesubgrain boundary starts to crack, as shown in figure9d, figure 12b andfigures13c and d. When the crack approaches to graphite, there are onlyone propagation path which is along the phase boundary between graphite and ferrite because of the oxidation, as shown in figure 13d.

Themorphology of the fatigue crack tipat 500^{o}C is shown infigure12b.It can be seen that the fatigue crack terminates in the ferrite,noobvious narrowed trend and much larger deflections appear.Since the ferrite has better resistance to oxidation[32],the results above can confirm that the crack is induced by the oxide layer. At the same time, theoxide layer and thegrain boundarycrackingappear.The latter may beexplained that oxidation preferentially spreads at the grain boundary, and the carbide precipitates at the grain boundary athigh temperatures.In summary, the

grain boundary weakens significantlyand then becomes the propagation channel of the crackat 500°C, whichis one of the reasons for the decrease of fatigue strength.

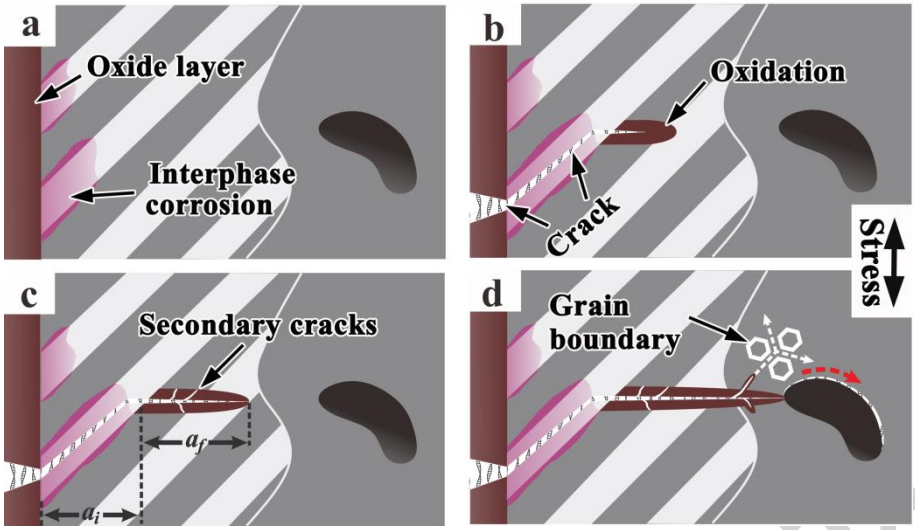

Figure 13.Schematic ofcrack formation and propagation at 500°C: (a) the oxide layer and interphase corrosion forming in the surface and the pearlite lamellae respectively; (b) oxide layercracking and oxidation propagating around the crack; (c) the secondary crack forming in the oxide layer; (d) grain boundary cracking and the crack propagating in the graphite.

4.2 Thestrengthening and damaging mechanism at high temperature

The fatigue crack propagation mode of the compacted graphiteiron changes at different temperatures. According to the phenomena observed in the experiment, the correspondingschematic illustrationof themicroscopic mechanismis shown in figure 14. The sample surface is oxidized with oxygen in the air at high temperature. The interphase corrosion occurring in the pearlite is one of the reasons in which the oxide layer penetrates into the matrix, as shown in figure 14a. There will be oxygen atom diffusion channelsdue to the alternating mixture ofthe cementite and ferrite plates. The corrosion potential difference between cementite and ferrite is the driving force of the interphase corrosion[30, 31]. In the corrosion process the cementite is protected but the ferrite is accelerated.Andeventually anoxide phase (Fe_2O_3,Fe_3O_4) forms,and then leads to crack initiation.

As mentioned above,the crack is produced prior to theoxide layerat 400°C,which providesa prerequisite for strengthening the material.The serrated flow phenomenon

in tensile stress-strain curves of compacted graphite iron appears at high temperatures, which could indicate the occurrence of dynamic strain aging.The effect of dynamic strain aging is considered to be a main reason for the improvement of fatigue strength of Fe-C alloy at 200-400^{o}C, as shown in figure 14b. There are two main mechanisms of dynamic strain aging. First of all, at high temperatures, the carbon atoms reach the activation energy and cluster to the surrounding dislocation, which hinders the dislocation slip and increases the fatigue life. Secondly, the carbon atoms are able to lock mobile edge dislocations which move during plastic deformation by gathering in their dilatation region [12]. This process increases the resistance to further dislocation movement by reducing the stored inner energy of the system and stabilizes the dislocation structure.

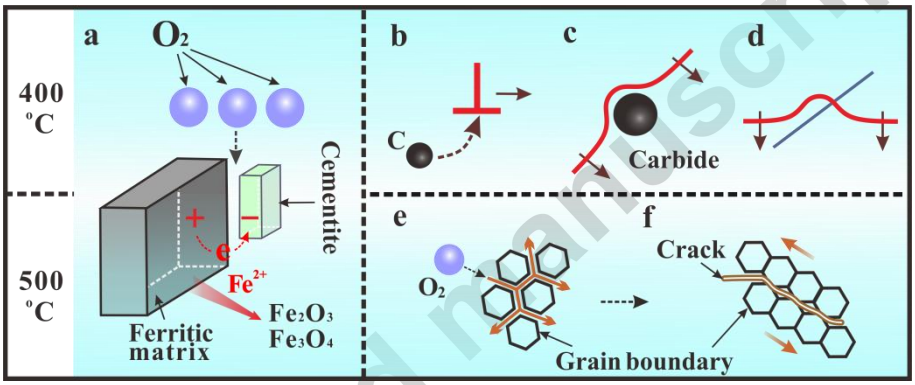

Figure 14.The strengthening anddamaging mechanisms of compacted graphite iron at high temperatures: (a) interphase corrosion; (b) dynamic strain aging; (c) precipitation strengthening; (d) dislocationstrengthening; (e)intergranular corrosion; (f) ferrite grain boundary sliding.

When the stress amplitude is higher than 160MPa, the fatigue livesat 400^{o}Care close to that at 25^{o}C, while below 160MPa,the fatigue lives at 400^{o}C improve obviously (figure4d).The reason for this phenomenon is probably due tothe competition between oxidation and dynamic strain agingat 400^{o}C.The interphase corrosion (oxidation) reduces the initiation life of the cracksignificantly, which results in a decrease in the overall fatigue life of the sample.However, the strengthening effect of dynamic strain aging may increase the fatigue life.At last the fatigue lives at 400 ^{o}C are close to that at 25 ^{o}C. On the other hand, when therange of stress

amplitudeis smaller, around 160MPa, the elastic strain of the oxide layer is below the critical value, the crack initiation lifewill be less affected by oxidation and the fatigue life will significantly improve due to the superposeddynamic strain aging effect.

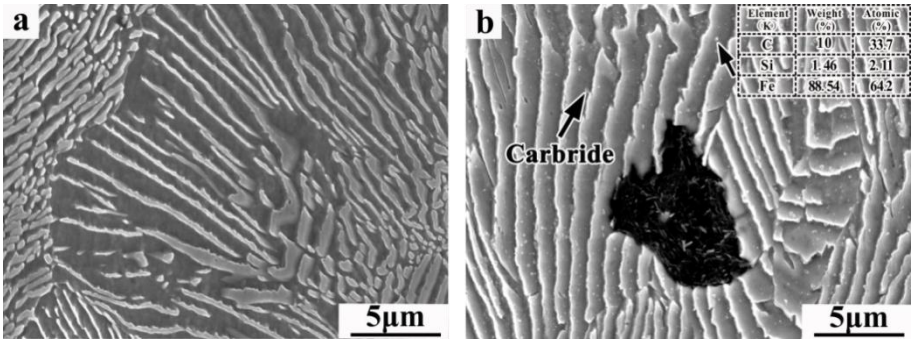

Figure15.Microstructure evolutions on longitudinal section of the fatigue fracture sample: (a) 25^{o}C, N_f=104766cycles; (b)400^{o}C, N_f=35522 cycles.

Meanwhile, a large number of carbides separate out fatigue fracture sample at 400 ^{o}C, as shown in figure 15b.As a comparison, the microstructure at 25^{o}C is shown in figure 15a; Thecarbide is a product of the diffusion of carbon atoms at high temperature.The precipitation of carbide with a high hardness can hinder the dislocation movement [33], and then prevent slip deformation, as shown in figure 14c. Both the dynamic strain aging and the precipitation of carbide will hinder the movement of dislocationsat the cracktip, resulting in the formation of dislocation strengthening, as shown in figure 14d.

At 500^{o}C, a large number of ferrite grain or subgrain boundaries star crackingto promote to form the main crack (figure 9d).Twomechanisms could be noticed.First of all, due to a large number of defects in the grain boundaries, the atoms are in the unstable state and easy to combine with oxygen to form inter-granular corrosion at high temperature, as shown in figure 14e.Secondary, at high temperature, due to the influence ofvacanciesdiffusion and grain boundary softening, the grain boundary will slide under the shear stress and form micro-cracks, as shown in figure 14f.

4.3 Influence of high temperature on fatigue strength

It is well known that the fatigue strength of the specimens is closely related to the theinitiation mechanism of fatigue crack[34, 35]. According to the above analysis, at room temperature, the fatigue crack of the compacted graphite iron mainly emerges at

the tip of the vermicular graphite. While at high temperatures,the oxidation promotes the crack to form primarily at the sample edge of the pearlite, and the crack propagation is due to the weakening effects of grain boundary at the crack tip.However, both the vermicular graphite and the oxide layer have played a separating role because of their low strengths.According to the research conducted by Tanaka et al.[36, 37], the relationship between fatigue crack thresholdstress(σ_{th}), threshold stress intensity factorrange(ΔK_{th}) and the crack size (a) has been deducedby analyzing the slip band blocked by thegrain boundary:

$$\sigma_{th} = \frac{K_c^m}{\sqrt{\pi(a+w_0)}} + \frac{2}{\pi}\sigma_{fr}^* cos^{-1}\left(\frac{a}{a+w_0}\right), \quad (5)$$

$$\Delta K_{th} = 2\sigma_{th}\sqrt{\pi a}. \quad (6)$$

Where, w_0 is lengthof slip band, $\sigma_{fr}^*$is friction stress of dislocation movement; K_c^m iscriticalstress intensity factor. When$a$ become zero, from Eq.(5)the fatigue strength of smooth specimencan be written as:

$$\sigma_e = \sigma_{fr}^* + \frac{K_c^m}{\sqrt{\pi w_0}}. \quad (7)$$

Since the Tanaka model can only be used at ambient temperature, it is necessary to modify further for use at high temperatures.

Because of the oxide layer is so brittle, it is assumed that there is no dislocation movement in the oxide and assuming that$\sigma_{fr}^* = 0$， $w_0$is equivalent to the criticalcrack lengtha_0, then formula (7) can be written as:

$$\sigma_e = \frac{K_c^m}{\sqrt{\pi a_0}} \quad (8)$$

substituting the formula (8) to the formulas (5) and (6),

$$\sigma_{th} = \frac{\sigma_e}{\sqrt{a/a_0+1}}, \quad (9)$$

$$\Delta K_{th} = \Delta K_0\sqrt{\frac{a}{a+a_0}}. \quad (10)$$

Where, $\Delta K_0 = 2\sigma_e\sqrt{\pi a_0}$, the range of intrinsic fatigue threshold stress intensity factor for cracks.

At high temperatures, the fatigue crack propagates into the matrix by the interphase corrosion. Therefore, the initial crack is determined by the length of the

interphase corrosion projected in a direction perpendicular to the stress in pearlite, where the crack size isa_i(figure 13c). The length of newly formed crack isthedistance perpendicular to the stressin pearlite lamellaea_f(figure13c),so the critical crack lengthshould be$a_i + a_f$.

$$\sigma_{-1} = \sigma_e \frac{1}{\sqrt{a_i/a_i+a_f + 1}}. \qquad (11)$$

Where, $\sigma_{-1}$is the fatigue strength.

The fitting result is shown in figure16. It can be seen that in ±15% error bands, the relationship between the fatigue strength and the ratio ofinterphase corrosion depth to critical crack lengthobeys Eq. (12),

$$\sigma_{-1} = 175.9 \times \frac{1}{\sqrt{a_i/a_i+a_f + 1}} \qquad (12)$$

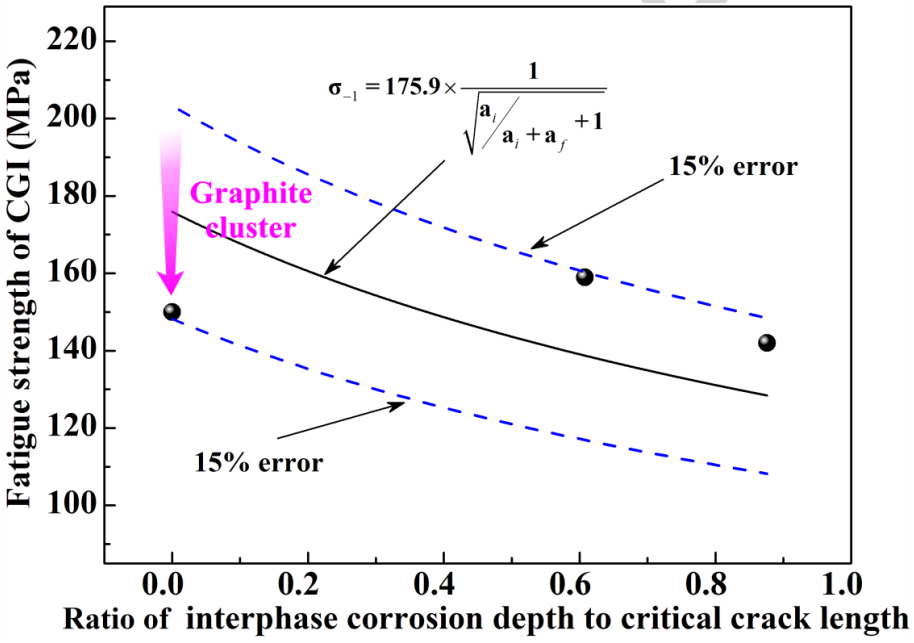

Figure 16.The fitting result between the fatigue strength and the ratio of interphase corrosion depthto critical crack length.

If the angle between pearlite lamellae andperpendicular to the stress directionisfixed, from the relationship, itcan be indicated that the fatigue strength ofcompacted graphite ironat high temperaturesmainly depends on the interphase corrosion lengthand pearlite lamellar spacing.In addition, due to the absence of

oxidation at room temperature, the phase corrosion depth can be understood as near-zero and then the fatigue strength should be the maximum. However, the difference between the measured value and the theoretical value is mainly due to the change of fatigue damage mechanism at room temperature. The fatigue crack initiation changes from the pearlite region to the graphite cluster. Therefore, the fatigue strength is rather below the theoretical value, which is also the reason for a larger standard error after fitting.

5. Conclusions

Based on the investigation of the effectof temperatures on high-cycle fatigue behavior and damage mechanismof compacted graphite iron,the following conclusions can be drawn：

1.With the increase of temperature, the tensile strength of compacted graphite irondecreases gradually; while the fatigue strengthincreasesat first and then decreases.

2. At 25 ^{o}C, the fatigue crack initiates from graphite debonding and propagates along the graphiteclusters. At high temperatures, the fatigue crack initiation life decreases due to the oxidation. However, the fatigue life at 400 ^{o}Cimproves owning to the dynamic strain aging effect. At 500 ^{o}C, the oxide layer induces the main crack to propagate to the matrix, which causes a decrease of fatigue strength coupled with the grain boundary softening.

3.Through the analysis ofdamage mechanism of compacted graphite ironat high temperatures, aquantitative relationship between the fatigue strength and the ratio of the interphase corrosion depth to the critical crack lengthstrengthwas proposed.

Acknowledge

The authors would like to thank Mr. G. Yao, Dr. C.H. Li and Mr. D. Tao for the fatigue experiment, SEM observation and ingot preparation. This work is supported

by National Natural Science Foundation of China (NSFC) under Grant No. 51331007.

References

[1] M. Konig, The influence of copper on microstructure and mechanical properties of compacted graphite iron, Cast Met. 22 (2009) 164-167.

[2] T. Sjogren, P. Vomacka, I.L. Svensson, Comparison of mechanical properties in flake graphite and compacted graphite cast irons for piston rings, Cast Met. 17 (2004) 65-71.

[3] M. Bazdar, H.R. Abbasi, A.H. Yaghtin, J. Rassizadehghani, Effect of sulfur on graphite aspect ratio and tensile properties in compacted graphite irons, J. Mater. Process. Techno. 209 (2009) 1701-1705.

[4] Q. Zhang, Z. Zuo, J. Liu, Failure analysis of a diesel engine cylinder head based on finite element method, Eng. Fail. Anal. 34 (2013) 51-58.

[5] V. Norman, P. Skoglund, D. Leidermark, J. Moverare, The effect of superimposed high-cycle fatigue on thermo-mechanical fatigue in cast iron, Int. J. Fatigue 88 (2016) 121-131.

[6] Y.H. Shy, C.H. Hsu, S.C. Lee, C.Y. Hou, Effects of titanium addition and section size on microstructure and mechanical properties of compacted graphite cast iron, Mater. Sci. Eng. A 278 (2000) 54-60.

[7] M. Selin, Tensile and thermal properties in compacted graphite irons at elevated temperatures, Metall. Mater. Trans. A 41 (2010) 3100-3109.

[8] Y. Qiu, J.C. Pang, E.N. Yang, S.X. Li, Z.F. Zhang, Transition of tensile strength and damaging mechanisms of compacted graphite iron with temperature, Mater. Sci. Eng. A 677 (2016) 290-301.

[9] J.C. Pang, S.X. Li, Z.G. Wang, Z.F. Zhang, General relation between tensile strength and fatigue strength of metallic materials, Mater. Sci. Eng. A 564 (2013) 331-341.

[10] J. Schijve, Fatigue of structures and materials, Kluwer Academic Publishers, Springer Netherlands , 2004.

[11] P.G. Forrest, Fatigue of Metals, Pergamon Press, Oxford, 1962.

[12] E. Kerscher, K.H. Lang, O. Vöhringer, D. Löhe, Increasing the fatigue limit of a bearing steel by dynamic strain ageing, Int. J. Fatigue 30 (2008) 1838-1842.

[13] S. Kim, S.L. Cockcroft, A.M. Omran, Optimization of the process parameters affecting the microstructures and properties of compacted graphite iron, J. Alloys Compd. 476 (2009) 728-732.

[14] S. Kim, S.L. Cockcroft, A.M. Omran, H. Hwang, Mechanical, wear and heat exposure properties of compacted graphite cast iron at elevated temperatures, J. Alloys Compd. 487 (2009) 253-257.

[15] S. Ghodrat, Thermo-mechanical fatigue of compacted graphite iron in diesel engine components, J. Bacteriol. 173 (2013) 2354-2365.

[16] X.S. Wang, W.Z. Zhang, Oxidation and thermal cracking behavior of compacted graphite iron under high temperature and thermal shock, Oxid. Met. 87 (2016) 1-10.

[17] Y. Qiu, J.C. Pang, S.X. Li, E.N. Yang, W.Q. Fu, M.X. Liang, Z.F. Zhang, Influence of thermal exposure on microstructure evolution and tensile fracture behaviors of compacted graphite iron, Mater. Sci. Eng. A 664 (2016) 75-85.

[18] C.G. Chao, T.S. Lui, M.H. Hon, A study of tensile properties of ferritic compacted graphite cast irons at intermediate temperatures, J. Mater. Sci. 24 (1989) 2610-2614.

[19] S. Kogoh, H. Ogino, T. Nakagawa, M. Kobayashi, K. Asami, Fatigue strength of spheroidal graphite cast iron at elevated temperatures under axial load, Int. J. Fatigue 12 (1990) 199-205.

[20] H. Aboulfadl, J. Deges, P. Choi, D. Raabe, Dynamic strain aging studied at the atomic scale, Acta Mater. 86 (2015) 34-42.

[21] S. Luo, S. Wu, Effect of dynamic strain aging on the microstructure and mechanical properties of a reactor pressure vessel steel, Mater. Sci. Eng. A 596 (2014) 25-31.

[22] B. Wang, P. Zhang, Q.Q. Duan, Z.J. Zhang, H.J. Yang, J.C. Pang, Y.Z. Tian, X.W. Li, Z.F. Zhang, High-cycle fatigue properties and damage mechanisms of pre-strained Fe-30Mn-0.9C twinning-induced plasticity steel, Mater. Sci. Eng. A 679 (2017)

258-271.

[23] S. Suresh, Fatigue of materials, Cambridge University Press, Cambridge, 1991.

[24] M.L. Roessle, A. Fatemi, Strain-controlled fatigue properties of steels and some simple approximations, Int. J. Fatigue 22 (2000) 495-511.

[25] J.C. Pang, M.X. Yang, G. Yang, S.D. Wu, S.X. Li, Z.F. Zhang, Tensile and fatigue properties of ultrafine-grained low-carbon steel processed by equal channel angular pressing, Mater. Sci. Eng. A 553 (2012) 157-163.

[26] X.H. An, S.D. Wu, Z.G. Wang, Z.F. Zhang, Enhanced cyclic deformation responses of ultrafine-grained Cu and nanocrystalline Cu–Al alloys, Acta Mater. 74 (2014) 200-214.

[27] Z.J. Zhang, P. Zhang, L.L. Li, Z.F. Zhang, Fatigue cracking at twin boundaries: Effects of crystallographic orientation and stacking fault energy, Acta Mater. 60 (2012) 3113-3127.

[28] W. Jiang, J. Dong, L. Wang, L. Lou, Effect of Casting Modulus on Microstructure and Segregation in K441 Superalloy Casting, J. Mater. Sci. Technol. 27 (2011) 831-840.

[29] P. Andresem, B. Antolovich, S.D. Antolovich, et al. ASM Handbook, Volume 19: Fatigue and Fracture, ASM International, 1996.

[30] A. Zhang, J. Xing, A quantitative investigation on the dynamic inter-phase corrosion of chromium white cast irons, Acta Metal. Sin. 37 (2007) 77-81.

[31] A.F. Zhang, J.D. Xing, L. Fang, J.Y. Su, Inter-phase corrosion of chromium white cast irons in dynamic state, Wear 257 (2004) 198-204.

[32] W.A.I. Baeslack, D.J. Duquette, W.F. Savage, Effect of ferrite content on stress corrosion cracking in duplex stainless steel weld metals at room temperature, Jpn. J. Pharmacol. 26 (1979) 504-6.

[33] D. Caillard, Dynamic strain ageing in iron alloys: The shielding effect of carbon, Acta Mater. 112 (2016) 273-284.

[34] J.C. Pang, Q.Q. Duan, S.D. Wu, S.X. Li, Z.F. Zhang, Fatigue strengths of Cu–Be alloy with high tensile strengths, Scripta Mater. 63 (2010) 1085-1088.

[35] J.C. Pang, S.X. Li, Z.G. Wang, Z.F. Zhang, Relations between fatigue strength

and other mechanical properties of metallic materials, Fatigue Fract. Eng. Mater. Struct. 37 (2014) 958-976.

[36] K. Tanaka, Y. Nakai, M. Yamashita, Fatigue growth threshold of small cracks, Int. J. Fracture 17 (1981) 519-533.

[37] Y. Qiu, Investigations on tensile and fatigue properties and damage mechanisms of compacted graphite irons used in diesel engine cylinder heads, Doctor thesis of University of Chinese Academy of Sciences,Shenyang,2017.